I.A.U
Karaj branch

Journal of
A p p l ied
C hemical
R esearch
jacr.kiau.ac.ir

Journal of Applied Chemical Research, 17, 2, 41-60 (2023)

Ultrasonic Assisted Adsorption of Rhodamine B (RhB) Dye by *Albizia Stem Bark Lebbeck* Modified by $Fe_2(MoO_4)_3$ Nanocomposite Synthesis: Experimental Design Methodology

Shiva Enolghozati[1], Nasrin Choobkar[1], Elham Pournamdari[2]*, Farzaneh Marahel[3]

[1]*Department of Environment, Kermanshah Branch, Islamic Azad University, Kermanshah, Iran*

[2]*Department of Chemistry, Islamshahr Branch, Islamic Azad University, Islamshahr, Iran*

[3]*Department of Chemistry, Omidiyeh Branch, Islamic Azad University, Omidiyeh, Iran*

(Received 14 Aug. 2022; Final revision received 16 Nov. 2022)

Abstract

The applicability of *Albizia Stem Bark Lebbeck* Modified by $Fe_2(MoO_4)_3$ nanocomposite synthesis for removing Rhodamine B dye from aqueous solutions has been reported. Identical techniques including BET, IR, XRD, EDX, and SEM have been utilized to characterize this novel material. Also, the impacts of variables including initial Rhodamine B dye concentration (X_1), pH (X_2), adsorbent dosage (X_3), and Sonication time (X_4) came under scrutiny using central composite design (CCD) under response surface methodology (RSM). The values of 10 mg L^{-1}, 0.025g, 6.0, 5.0 min were considered as the ideal values for Rhodamine B dye concentration, adsorbent mass, pH value, and contact time respectively. The adsorption equilibrium and kinetic data were fitted with the Langmuir isotherm model and pseudo-second-order kinetics (R^2: 0.999) with maximum adsorption capacity (q_{max}: 98.0 mgg^{-1}) respectively. Thermodynamic parameters (R^2: 0.998, $\Delta G°$: -95.58 kJ mol^{-1}, $\Delta H°$: -29.24 kJ mol^{-1}, $\Delta S°$: -131.49 kJ mol^{-1} K^{-1}) also indicated Rhodamine B dye adsorption is feasible, spontaneous and exothermic. The overall results confirmed that *Albizia Stem Bark Lebbeck* Modified by $Fe_2(MoO_4)_3$ nanocomposite could be a promising adsorbent material for Rhodamine B dye removal from aqueous solutions.

Keywords: Rhodamine B (RhB) dye, Adsorption, Isotherms, Central Composite Design (CCD), Response Surface Methodology (RSM).

**Corresponding author:* *Elham Pournamdari, Department of Chemistry, Islamshahr Branch, Islamic Azad University, Islamshahr, Iran. Email: epournamdar@iiau.ac.ir.*

Introduction

Industrialization and accelerated urbanization are found to be the major reasons for water pollution in developing countries [1]. Wastewaters from industries like textile, paper, rubber, plastic, leather, cosmetic, food, and drug industries contain dyes and pigments which are hazardous and can cause allergic dermatitis, skin irritation, cancer due to the colorization of the water [2,3]. Most dyes possess complex aromatic structures and resistant to aerobic and anaerobic conditions, heat, light, and oxidation. Besides water bodies, these dyes can penetrate into the soil and contaminate groundwater aquifers [4]. During the past few years, there has been an increasing concern regarding the residual dye in textiles, as it will be released into the environment. These problems make an emergency to design and develop new protocols to treat them and achieve a safe and clean media [5,6].

Rhodamine B is one of the most widely used synthetic dyes. It is an organic chloride salt of N-[9-(2-carboxyphenyl)-6-(diethylamino)-3H-xanthen-3ylidene]-N-ethylethanaminium that shows structured (RhB) dye in Figure 1. Its ingestion causes ill effect on nose, skin, eyes, tongue, respiratory tract, reproductive system failure etc. [7,8]. Therefore, the removal of dyes (Rhodamine B) before the discharge into aquatic systems is required to safeguard human and ecosystem health.

Various treatment methods have been utilized for the removal of dyes from contaminated wastewater, including advanced oxidation processes, catalytic degradation, adsorption and electrochemical degradation. Among these methods, adsorption is a promising approach owing to its simple operational design, non-susceptibility to pollutants, reusability, high efficiency, low cost, and relatively low waste production [9].

The adsorption method is especially suitable for solving dyes, environmental, gases and metals problems and has many advantages to become the focus and hot spot of research. Adsorption is one of the best and simplest techniques for the removal of toxic and noxious impurities in comparison to other conventional protocols such as flocculation, membrane filtration, advanced oxidation, ozonation, photocatalytic degradation, and biodegradation [10-13]. The physical and chemical properties of an adsorbent determine the effectiveness of an adsorption process extremely. The valuable properties are considered as follows: having high adsorption capacity, being available and recoverable, and also being economical.

In recent years, it was tried to eliminate specified organics from water samples by applying diverse potential adsorbents. In this connection, magnetic nanoparticles (MNPs) as unique adsorbents thanks to their small diffusion resistance, high adsorption capacity, and large surface area have extensively been noticed. Their application for instance, in the separation of

chemical species like dyes, environmental pollutants, gases, and metals has proven to be successful [14,15]. Synthesis of coupling of sorbent with any oxide@ferric nanocomposite including a large surface area, being widely accessible, being stable in an acidic/basic environment, and having a stable structure at high temperatures one of the most widely used nanocomposites is the adsorption process [16-19].

Albizia Stem Bark Lebbeck tree grows in many regions. This sorbent is derived from *Albizia Stem Bark Lebbeck* as the most important of all non-toxics. Fast and clean synthesis without the use of toxic and dangerous compounds or surfactants made it a highly stable and reusable ecofriendly sorbent under solvent-free condition and excellent yield. The application of *Albizia Stem Bark Lebbeck* modified by $Fe_2(MoO_4)_3$ nanocomposite sorbent for Rhodamine B dye measurement is juxtaposed against other commercial sorbents [20,21].

The *Albizia Stem Bark Lebbeck* modified by $Fe_2(MoO_4)_3$ nanocomposite as a novel adsorbent is simply synthesized and subsequently characterized by scanning electron microscopy (SEM), Fourier transform infrared spectroscopy (FTIR) and X-ray diffraction (XRD) analysis. The experimental conditions of pH of solution, contact time, initial (RhB) dye concentration, adsorbent dosage and the dye removal percentage, were investigated and optimized by central composite design (CCD) under response surface methodology (RSM). It was shown that the adsorption of (RhB) dye follows the pseudo-second-order rate equation. The Langmuir model was found to be applied for the equilibrium data explanation. It was shown through the study of Kinetic models (both pseudo-first-order, pseudo-second-order diffusion models) that the kinetic of adsorption process is controlled by the pseudo-second-order model. The capability of *Albizia Stem Bark Lebbeck* modified by $Fe_2(MoO_4)_3$ nanocomposite in eliminating of (RhB) dye from wastewater treatment was demonstrated by evidence.

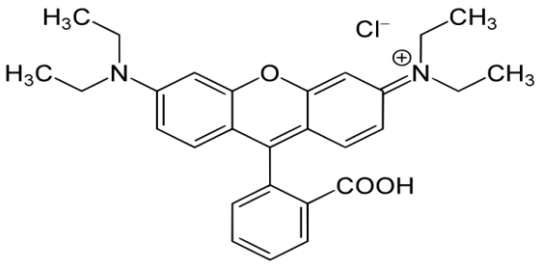

Figure 1. The structures of Rhodamine B (RhB) dye.

Experimental

Materials and Instrumentation

All the chemicals used are of the highest purity and purchased from Merck (Darmstadt, Germany). Rhodamine B (RhB) dye (99%), Ammonium heptamolybdate (99%), and Iron nitrate (III) (98.0%). The standard and experimental solutions were obtained by diluting the stock solutions with deionized water. The applied instruments were as follow: spectrophotometer model 1601 PC (Shimadzu Company, Japan). IR spectra were registered on a (PerkinElmer company, Germany). SEM (Phillips, PW3710, Netherland), used to study the morphology of samples. An ultrasonic bath with a heating system (Tecno-GAZ SPA Ultra Sonic System, Italy) was used for the ultrasound-assisted adsorption procedure.

Preparation of Albizia Stem Bark Lebbeck m*odified by $Fe_2(MoO_4)_3$ nanocomposite*

The iron oxide-molybdenum nanocomposite was prepared in a synergistic process by mixing the juice solutions of heptemolybdate ammonium and iron nitrate. Ammonium heptamolybdate ($[NH_4]_6Mo_7O_{24}.4H_2O$]) was charged into 175 ml distilled water disintegrated solution and the pH of the solution was adjusted to 1.8 with concentrated chloride. A solution containing 50 grams of iron nitrate [$Fe(NO_3)_3.4H_2O$] with 350 milliliters of deionized distilled water was obtained. The container with the heptamol dilution of ammonium was positioned in warm bath with temperature of 70°C. The iron nitrate solution was added slowly while stirring the ammonium heptamolybdate solution. Then the bath temperature was increased to 90°C. The sediment suspension was stirred for 3 hours. Stirring was stopped and the suspension was placed in the laboratory for 2 hours. The *Albizia Stem Bark Lebbeck* modified by $Fe_2(MoO_4)_3$ nanocomposite was produced from a *Albizia Stem Bark Lebbeck* with an equal weight ratio and after analysis with BET, FT-IR, XRD and SEM was utilized as an adsorbent [21,22].

Adsorption method

The elimination of (RhB) dye in an adsorption combined with *Albizia Stem Bark Lebbeck* modified by $Fe_2(MoO_4)_3$ nanocomposite in erlenmeyer flask was loaded with exact quantities of (RhB) dye solution (50 mL) at specified concentration 10 mg L^{-1}, and pH of 6.0 with a known quantity of adsorbent (0.025 g) while the desired sonication time (5 min) was maintained at the 25^{o}C [23]. The adsorption trials were executed in mode and the solution was ultrasonicated at conditions devised under RSM. The analysis of the dilute phase was done for determining (RhB) dye concentration with the help of UV–Vis spectrophotometer

model 1601 PC, set at wavelengths 620 nm. The computation of the removal percentage of (RhB) dye during a given period and the calculation of the amount of (RhB) dye adsorbed after reaching the equilibrium (qe (mg/g)) was done using the ensuing equations:

$$R\% = \frac{C_{0i} - C_{ei}}{C_{0i}} \times 100 \quad (1)$$

$$q_i = \frac{V(C_{0i} - C_{ei})}{M} \times 100 \quad (2)$$

C_0 (mg L^{-1}) in the formula refers to the initial (RhB) dye concentration and C_e (mg L^{-1}) represents the equilibrium (RhB) dye concentration in aqueous solution. V (L) shows the solution volume and W (g) signifies the mass adsorbent [24].

Central composite design (CCD)

The central composite design as most applicable type of RSM was applied for modelling and the optimization of effects of concentration of (RhB) dye (X_1), pH (X_2), amount of adsorbent (X_3) and contact time (X_4) on the ultrasonic-assisted adsorption of (RhB) dye by *Albizia Stem Bark Lebbeck* modified by $Fe_2(MoO_4)_3$ nanocomposite [24]. Four independent variables were set at four levels at which the R% of (RhB) dye as response was determined and shown in (Tables 1-3) [25].

Table 1. Experimental factors, levels and matrix of CCD.

Factors	**levels**			**Star pointα = 2.0**	
	Low (-1)	Central (0)	High (+1)	-α	+α
(X_1) (RhB) dye conc. (mg L^{-1})	10	15	20	5	25
(X_2) pH	5.0	6.0	7.0	4.0	8.0
(X_3) Adsorbent mass (g)	0.015	0.025	0.035	0.005	0.045
(X_4) Sonication time (min)	3.0	4.0	5.0	2.0	6.0

Table. 2. The design and the response.

Run	**X_1**	**X_2**	**X_3**	**X_4**	**R% (RhB) dye**
1	10	6	0.025	4	92.6
2	20	7	0.015	3	55.0
3	10	7	0.025	5	95.0
4	20	6	0.025	4	92.5
5	30	5	0.015	3	73.0
6	10	7	0.035	4	99.2
7	20	4	0.025	4	96.0

8	20	6	0.025	6	93.0
9	20	5	0.035	3	80.0
10	20	5	0.025	5	90.0
11	20	6	0.025	4	93.2
12	20	7	0.015	5	70.7
13	20	7	0.035	5	80.4
14	10	7	0.015	3	95.0
15	10	6	0.025	4	93.0
16	20	5	0.035	5	93.5
17	20	6	0.025	4	93.0
18	10	7	0.025	3	93.6
19	10	6	0.030	5	97.6
20	10	5	0.035	5	95.0
21	10	6	0.025	5	100.0
22	20	6	0.025	4	58.7
23	10	7	0.035	2	65.0
24	20	6	0.025	4	93.6
25	10	7	0.03	4	93.51
26	20	6	0.005	4	90.0
27	20	6	0.025	2	75.0
28	20	8	0.025	4	82.0
29	10	7	0.030	4	95.0
30	10	6	0.025	5	100.0

Table 3. Characterization Analysis BET of sorbent.

Characterization		**Samples**	
		Albizia Stem Bark Lebbeck	***Albizia Stem Bark Lebbeck* modified by $Fe_2(MoO_4)_3$**
	Correlation Coefficient	0.9972	0.9915
BJH desorption	Surface area (m^2/g)	45.84	45.17
	Pore volume (cm^3/g)	0.9202	0.8917
BJH adsorption	Surface area (m^2/g)	90.27	89.80
	Pore volume (cm^3/g)	0.9493	0.9288

Results and discussion

BET analysis of Albizia Stem Bark Lebbeck Modified by $Fe_2(MoO_4)_3$ nanocomposite

The Brunauer–Emmett–Teller (BET) analysis was used for determination of surface area of the *Albizia Stem Bark Lebbeck* Modified by $Fe_2(MoO_4)_3$ nanocomposite by N_2 adsorption before and after (RhB) dye adsorption (Figure 2). The decrease of surface area indicates that (RhB) dye is almost in almost all *Albizia Stem Bark Lebbeck* modified by $Fe_2(MoO_4)_3$ nanocomposite pores after absorption. The adsorption capacity with an increase in the number of adsorbed $Fe_2(MoO_4)_3$ nanocomposites, the relative partial pressure range on the adsorption isotherms gradually decreases. This is because the $Fe_2(MoO_4)_3$ nanocompsite, in the composite spread into *Albizia Stem Bark Lebbeck* channels, made the channels narrow and the pore volume decrease.

The gradual decrease of BET specific surface area indicates that the $Fe_2(MoO_4)_3$ nanocompsite, and has entered the *Albizia Stem Bark Lebbeck* pores rather than adsorbed on the outer surface of the *Albizia Stem Bark Lebbeck*. By comparing the pore size distribution of the samples, it can be seen that with the increase of gradually the increase of the number of adsorbed $Fe_2(MoO_4)_3$ nanocompsite, the most probable pore diameter is gradually reduced. This is because when the $Fe_2(MoO_4)_3$ nanocompsite, was introduced into the *Albizia Stem Bark Lebbeck* channels, the most probable pore diameter reduced, indicating that the $Fe_2(MoO_4)_3$ nanocompsite, entered the *Albizia Stem Bark Lebbeck* channels [26].

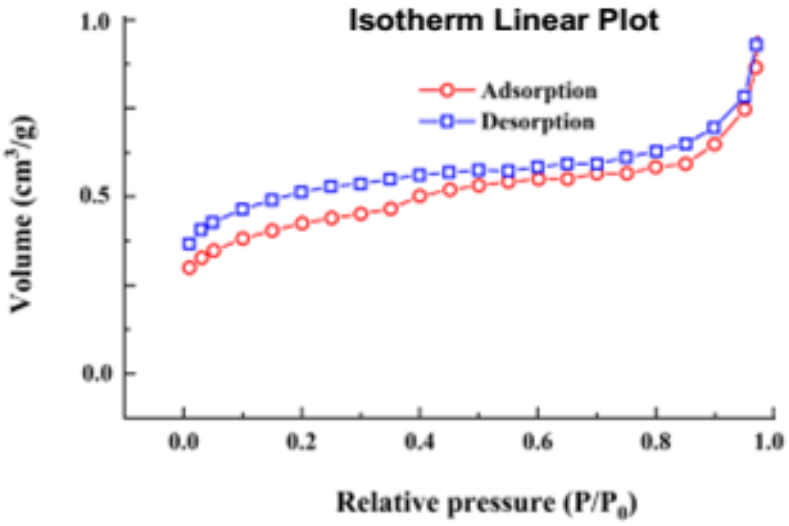

Figure 2. N_2 gas adsorption/desorption isotherms of *Albizia Stem Bark Lebbeck* and *Albizia Stem Bark Lebbeck* Modified by $Fe_2(MoO_4)_3$ nanocomposite.

IR, XRD and EDX analysis

The IR spectra of *Albizia Stem Bark Lebbeck* and *Albizia Stem Bark Lebbeck* Modified by $Fe_2(MoO_4)_3$ nanocomposite in the 500–4000 cm^{-1} wave number range, as demonstrated in Figure 3a, the IR spectrum of *Albizia Stem Bark Lebbeck* modified by $Fe_2(MoO_4)_3$ nanocomposite presents clear peak at 776.5 cm^{-1} related to Fe–O. The peak at 3415 cm^{-1} can be attributed to –OH stretching [22,27]. Different X-ray emission peaks are *Albizia Stem Bark Lebbeck* modified by $Fe_2(MoO_4)_3$ nanocomposite at 62.0(440), 56.0(511), 44.75(400), 38.2(311), 33.0(220) and 21.45(111), shown in (Figure 3b). The signal at $2\theta = 38.2^{\circ}$ (311) is ascribable to diffractions and reflections from the carbon atoms. The positions of diffraction peaks are in agreement with the standard samples [28]. EDX (energy-dispersive X-ray spectroscopy) spectrum of (Figure 3c) The EDX transmittance spectrum of the prepared *Albizia Stem Bark Lebbeck* and (Figure 3d) EDX spectrum recorded from a film, after the formation of *Albizia Stem Bark Lebbeck* modified by $Fe_2(MoO_4)_3$ nanocomposite [27,28].

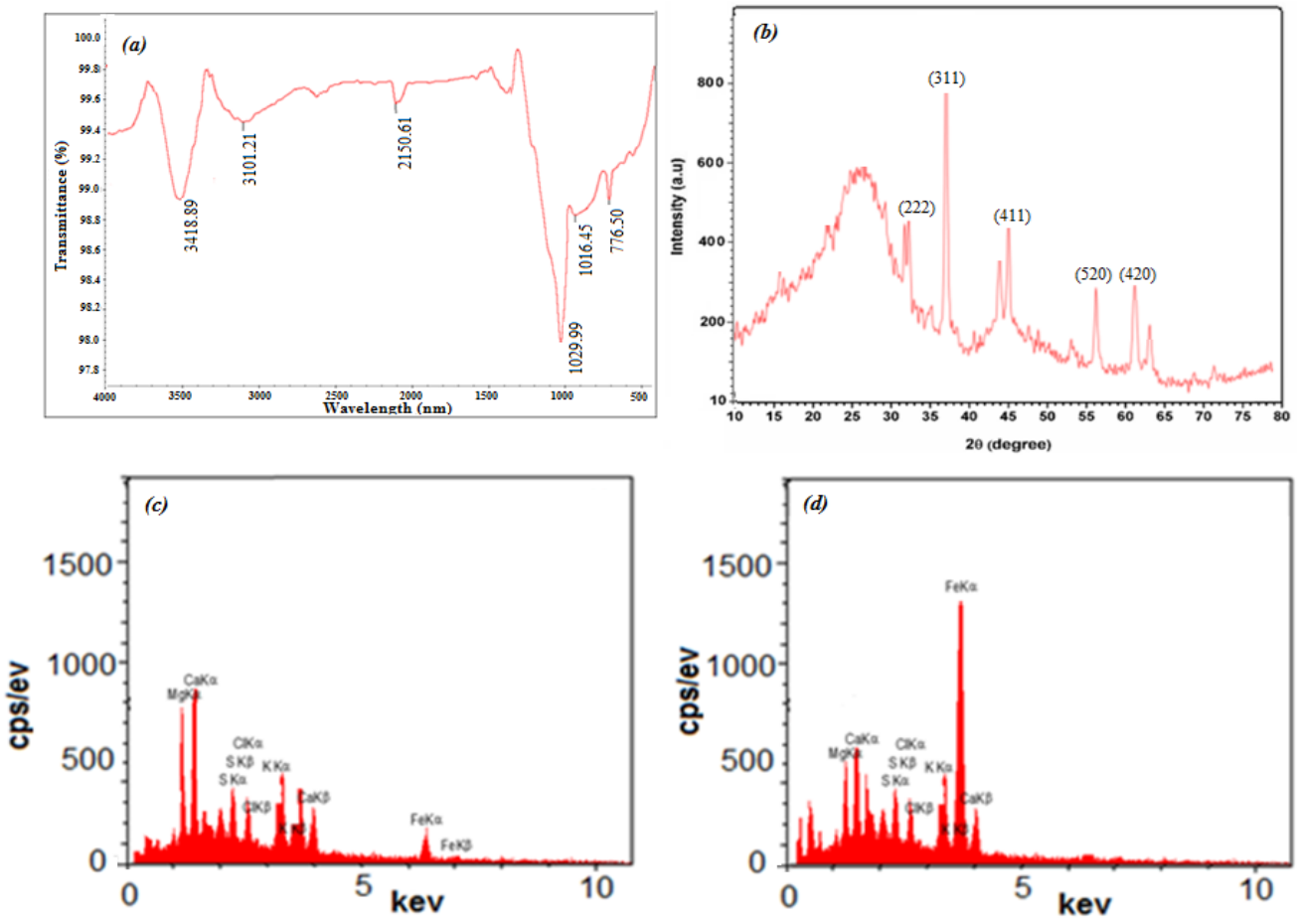

Figure 3. (a) The IR spectrum (b) XRD pattern of *Albizia Stem Bark Lebbeck* modified by $Fe_2(MoO_4)_3$ nanocomposite. (c) The EDX transmittance spectrum of the prepared *Albizia Stem Bark Lebbeck* and (d) The EDX transmittance spectrum of the prepared *Albizia Stem Bark Lebbeck* modified by $Fe_2(MoO_4)_3$ nanocomposite.

Surface morphology

The morphological properties of *Albizia Stem Bark Lebbeck* modified by Fe_2 $(MoO_4)_3$ nanocomposite were investigated by SEM and is exhibited in (Figure 4), It can be seen that the particles are mostly spherical with various size, in the range of 40-60 nm very close to that determination by XRD analysis [21,29].

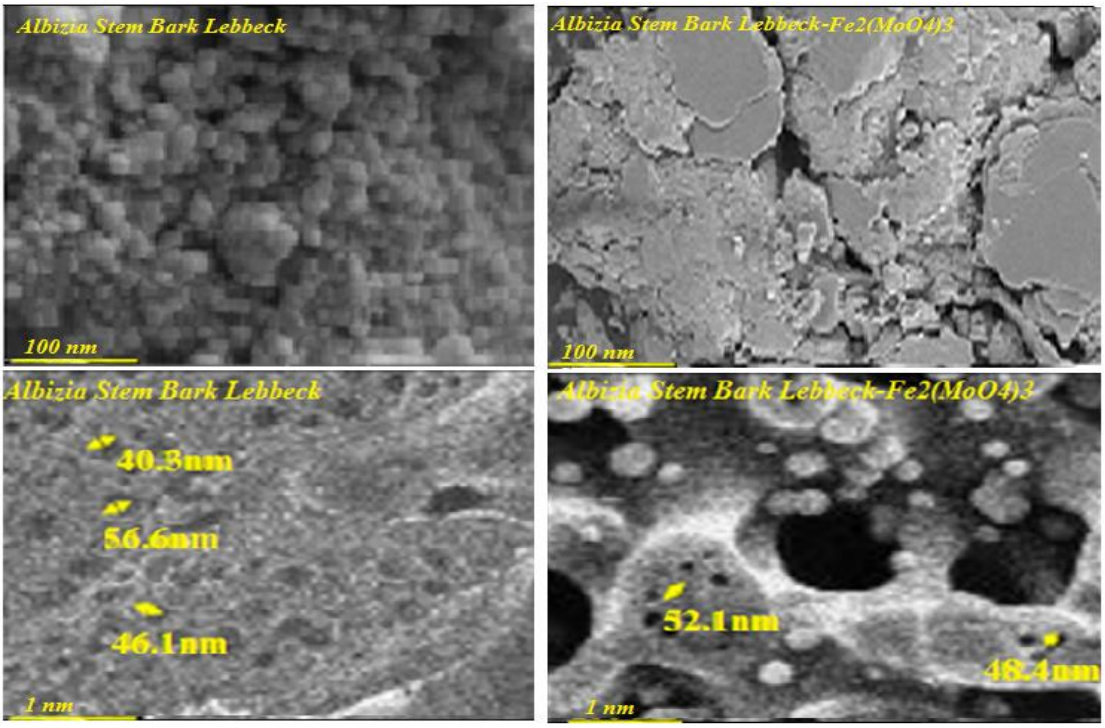

Figure 4. The SEM image of the prepared *Albizia Stem Bark Lebbeck* modified by Fe_2 $(MoO_4)_3$ nanocomposite in 100 nm and 1nm.

Modeling the process and statistical analysis

The variance analysis of all the linear, quadratic and interaction impacts of the three planning factors in relation to R% of (RhB) dye is represented in (Table 4). By considering the value of the determination coefficient for deleting (RhB) dye, it has been noticed that the response surface quadratic model was a befitting model for predicting the function of (RhB) dye adsorption on *Albizia Stem Bark Lebbeck* modified by Fe_2 $(MoO_4)_3$ nanocomposite [30]. The represents Eqs. (3), codified values for the quadratic equations after ruling out the insignificant terms.

$$R\%_{(RhB)\ dye} = 93/084 - 10/093X_1 - 3/340X_2 + 2/4167X_3 + 4/2700X_4 - 4/9075X_1X_2 - 1/3925X_1X_3 + 3/5525X_1X_4 + 0/89500X_2X_3 - 0/17500X_2X_4 - 0/44000X_3X_4 - 3/7119X_1^2 - 1/1059X_2^2 + 0/39410X_3^2 - 2/3559X_4^2 \quad \text{Eqs. (3)}$$

The value of the determination coefficient for deleting (RhB) dye in (Table 4), it has been noticed that the response surface quadratic model was a befitting model for predicting the function of (RhB) dye adsorption on *Albizia Stem Bark Lebbeck* modified by $Fe_2 (MoO_4)_3$ nanocomposite.

Table 4. Analysis of Variance for full quadratic model.

			(RhB) dye		
Source of variation	**Df**	**Sum of square**	**Mean square**	**F-value**	**P-value**
Model	14	4353.1	310/93	751.23	< 0.0001
X_1	1	1746.2	1746.2	4218.9	< 0.0001
X_2	1	267.73	267.73	646.86	< 0.0001
X_3	1	140.17	140.17	338.65	< 0.0001
X_4	1	437.59	437.59	1057.2	< 0.0001
X_1X_2	1	385.34	385.34	930.99	< 0.0001
X_1X_3	1	31.025	31.025	74.957	< 0.0001
X_1X_4	1	201.92	201.92	487.86	< 0.0001
X_2X_3	1	12.816	12.816	30.965	< 0.0001
X_2X_4	1	0.49	0.49	1.1839	0.29375
X_3X_4	1	3.0976	3.0976	7.4839	0.015321
X_3X_5	1	225.83	225.83	545.61	< 0.0001
X_1^2	1	33.962	33.962	82.053	< 0.0001
X_2^2	1	4.3128	4.3128	10.42	0.0056318
X_3^2	1	154.12	154.12	372.37	< 0.0001
X_4^2	15	6.2085	0.4139	751.23	< 0.0001
Residual	9	5.1621	0.57357		
Lack of Fit	6	1.0464	0.1744	3.2889	0.080484
Pure Error	29	3251.3			
Cor Total					

Response surface methodology (RSM) analysis

The 3D-RSM surfaces corresponding to R% (RhB) dye were depicted and considered to optimize the significant factors and to give useful information about the possible interaction of variables. As also seen from Figure 5, the effects of significant interaction terms on the curvature of the surfaces are observed as expected the RSM plot (Figure 5), that the dye removal percentage changes versus the adsorbent dosage [13,31]. The positive increase in the dye removal percentage with increase in adsorbent mass is seen. Significant diminish in

removal percentage at lower amount of *Albizia Stem Bark Lebbeck* modified by $Fe_2(MoO_4)_3$ nanocomposite is attribute to higher ratio of dye molecules to the vacant sites of the adsorbent. The maximum (RhB) dye deletion of 100%, the optimum conditions were as follows: pH of 6.0, ultrasound time of 5 min, adsorbent mass of (0.025 g) and initial (RhB) dye equal to 10.0 mg L^{-1} for (RhB) dye. Additionally, to examine the optimum conditions experimentally, eleven experiments under the same conditions at 25^0C was conducted. Based on the great conformity between the experimental and prediction data, it was confirmed that the central composite design could be utilized successfully for the evaluation and optimization of the influences of the adsorption independent variables on the removal efficiency of (RhB) dye from aqueous media with the help of *Albizia Stem Bark Lebbeck* modified by $Fe_2(MoO_4)_3$ nanocomposite [32,33].

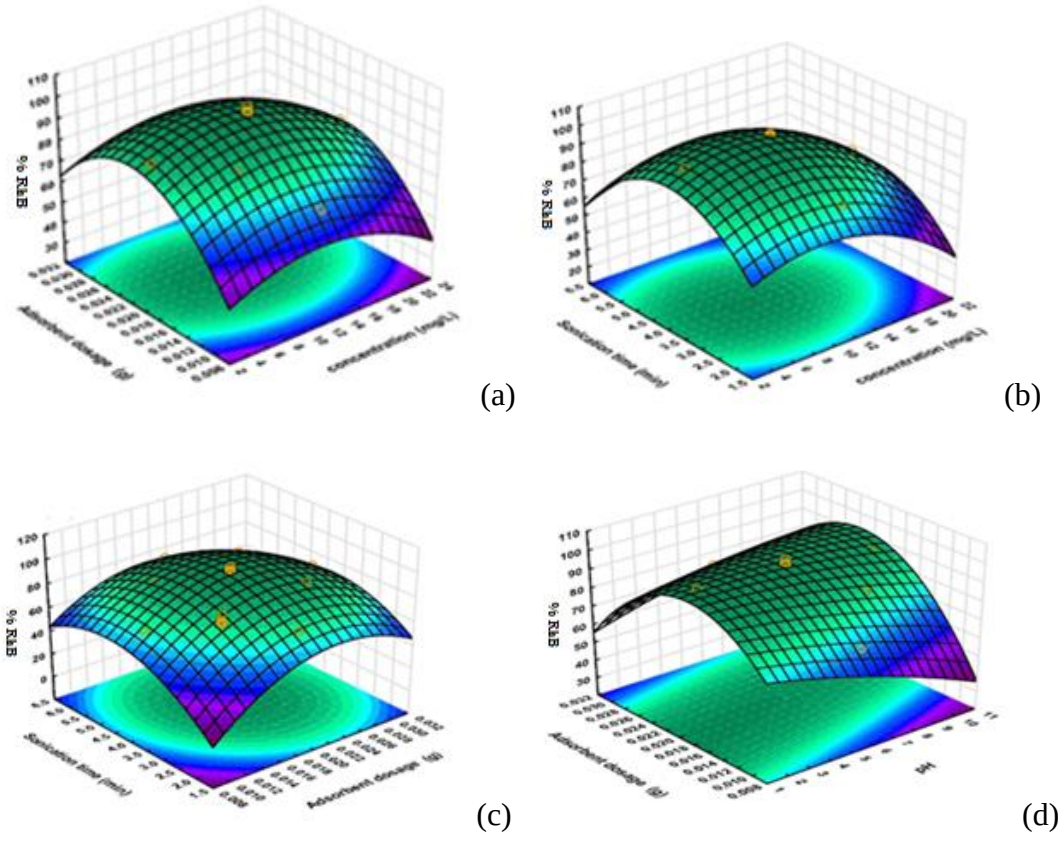

Figure. 5. Response surfaces for the (RhB) dye removal: (a) adsorbent dosage - initial (RhB) dye concentration (b) contact time, initial (RhB) dye concentration (c) contact time - adsorbent dosage (d) (RhB) dye adsorbent dosage (RhB) dye – pH.

Optimization of CCD

The profile for the desirable option with predicted values in the STATISTICA 10.0 software was used for the optimization of the process in Figure 6. The based on the great conformity

between the experimental and prediction data, it was confirmed that the central composite design could be utilized successfully for the evaluation and optimization of the influences of the adsorption independent variables on the removal efficiency of (RhB) dye from aqueous media with the help of *Albizia Stem Bark Lebbeck* modified by $Fe_2(MoO_4)_3$ nanocomposite.

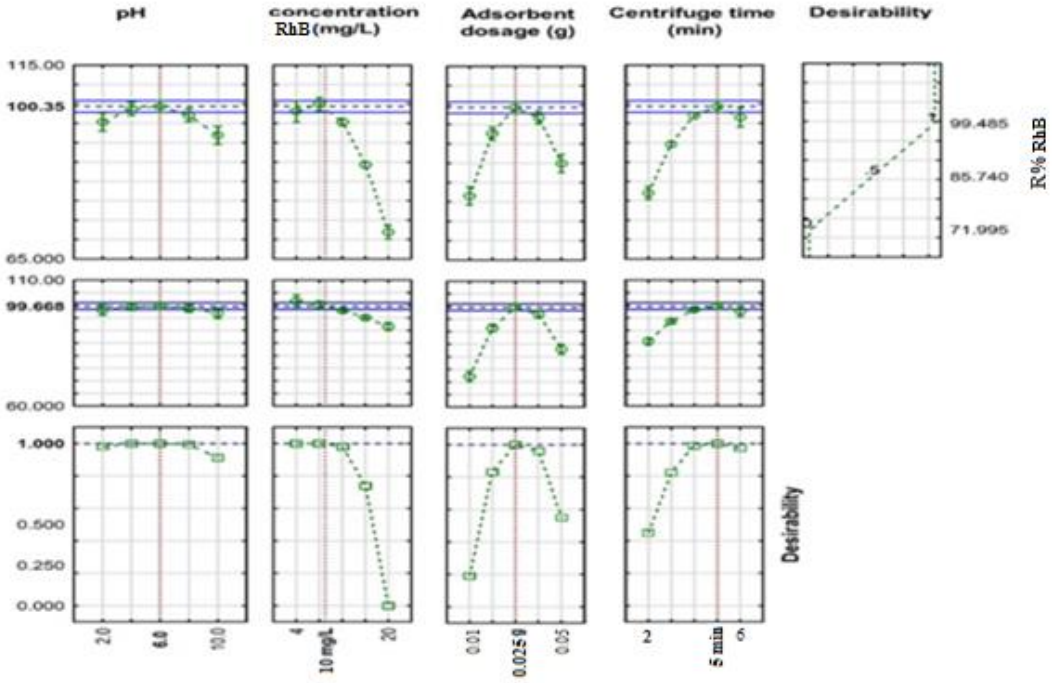

Figure 6. Profiles values for removal of (RhB) dye after optimization.

Adsorption isotherms

The equilibrium adsorption analysis is important to find out the adsorption levels at a specific adsorbate concentration and to underpin the further types of adsorption followed. The experiments were conducted by varying the contact time and evaluating the equilibrium adsorbate concentration (C_e) and equilibrium adsorption capacity (q_e). The obtained data were analyzed by established adsorption isotherm models [34,35]. Langmuir adsorption isotherm model confirmed the lack of any interaction amongst adsorbed molecules and the adsorption process on uniform surfaces. Langmuir model is defined in the following equation [36]:

$$\frac{C_e}{q_e} = \frac{1}{K_L q_{\max}} + \frac{1}{q_{\max}} C_e \quad (4)$$

In relation (4) q_m: is the value of monolayer adsorption capacity in Langmuir model and K_L: constant value of Langmuir (mg L^{-1}). Increasing the amount of adsorbent caused a

considerable increase in the adsorbed ions amounts in Table 5. Freundlich isotherm model is the more for the adsorption of components dissolved in a liquid solution, it is assumed that: First, the adsorption is monolayer and chemical, and second, the energy of the adsorption sites is not the same, is the adsorbent surface is not uniform [37]:

$$\ln q_e = \ln K_F + \frac{1}{n} \ln C_e \quad (5)$$

K_F and n are experimental constants where K_F is in terms of $((mg)^{1-n}\ L^n g^{-1})$ and is proportional to the adsorption capacity, and n is a unit less quantity and shows the intensity of adsorption with a range between 0.1 to 1.0. The calculation of K_F and adsorption capacity in the Freundlich model is shown in (Table 5). Temkin isotherm is the indirect interaction between adsorbate and adsorbent base on following equation:

$$q_e = \frac{Rt}{b} ln\ K_T + \frac{RT}{b} lnC_e \quad (6)$$

In this model as mentioned above, R, b, t, K_T and T are the universal gas constant (8.314 J mol^{-1}. K^{-1}), Temkin constant, the heat of the adsorption (J mol^{-1}), the binding constant at equilibrium (L mg^{-1}) and absolute temperature (K) In Table 5 [38].

Table 5. The adsorption isotherm models of (RhB) dye onto *Lebbeck* Modified by $Fe_2(MoO_4)_3$ nanocomposite. [C_0= 10.0 mg L^{-1}, pH = 6.0, dosage sorbent = 0.025 g, t_c = 5.0 min, T=25^{0}C].

Isotherm	Equation	parameters	R% (RhB) dye
Langmuir	$q_e=q_m bC_e/(1+bC_e)$	q_m (mgg^{-1})	98.0
		K_L (L mg^{-1})	0.487
		R^2	0.9911
Freundlich	$\ln q_e = \ln K_F + (1/n) \ln C_e$	1/n	0.55
		K_F $(mg)^{1-n}$ L^n g^{-1}	4.09
		R^2	0.9829
Temkin	$q_e = B_1 \ln K_T + B_1 \ln C_e$	B_T (J mol^{-1})	14.15
		K_T (L mg^{-1})	6.855
		R^2	0.9634

The adsorption kinetics survey

Kinetic models help in understanding the mechanism of dyes adsorption and evaluate the performance of various adsorbents for the removal of dyes. Among the many kinetic models developed mostly used are the Lagargren's pseudo-first order kinetics and pseudo-second order model [39,40]. The quasi-first-order kinetic model formula is:

$$\ln(q_e - q_t) = \ln q_e - \frac{k_1}{2.303} t \ (7)$$

The quasi-second-order dynamic model formula is:

$$\frac{t}{q_t} = \frac{1}{k_2 q_e^2} + \frac{t}{q_e} \ (8)$$

Where qt and qe are the sorption quantity at time t and equilibrium respectively, k is the rate constant. Thus a plot of t/ q via t gives the pseudo-second order adsorption. Pseudo second-order rate constant was determined from the respective plots. From the experimental results, it was found that the removal of (RhB) dye follows pseudo-second order rate shown in (Table 6) [41].

Table 6. Various Kinetic constants and their correlation coefficients calculated for the adsorption of (RhB) dye onto *Lebbeck* Modified by $Fe_2(MoO_4)_3$ nanocomposite. [C_0= 10.0 mg L^{-1}, pH = 6.0, dosage = 0.025 g, t_c = 5.0 min, T=25^{0}C].

Models	parameters	R% (RhB) dye
pseudo-First-order kinetic	$k_1(min^{-1})$	0.987
	q_e (mgg^{-1})	17.92
	R^2	0.9894
pseudo-Second-order kinetic	k_2 (min^{-1})	0.154
	q_e (mgg^{-1})	15.56
	R^2	0.9995
q_{exp} (mgg^{-1})		102.5

Adsorption thermodynamics

Temperature is one of the most important factors in dyes removal efficiency by focusing on change in nature of the reaction (exothermic or endothermic) to reveal spontaneous and non-spontaneous reaction. Thermodynamic parameters can be using the Eqs. (9) and (10) [42,43].

$$\Delta G^\circ = -RT \ln K_{ad} (9)$$

$$\ln K_{ad} = \frac{-\Delta H^\circ}{RT} + \frac{\Delta S^\circ}{R} (10)$$

Where, T is the temperature in Kelvin, R the gas constant (8.314 J/mol. K), ΔS° and ΔH° values can also be determined from the slope and intercept of the plot of Ln K^0 values 1/T, respectively (Table 7). The Gibbs free energy (ΔG^0 degree of spontaneity of the adsorption process and the low values reflect an energetically favorable adsorption process. The negative value of (ΔH°) confirms that the sorption process was exothermic in nature and a given amount of heat is evolved during the binding of (RhB) dye onto *Albizia Stem Bark Lebbeck*

modified by $Fe_2 (MoO_4)_3$ nanocomposite the surface of adsorbent. The highly negative ΔS^0 values indicate significant decrease in the degree of randomness at solid/liquid interface during the sorption process [44].

Table 7. The thermodynamic parameters for the adsorption of (RhB) dye onto *Lebbeck* Modified by $Fe_2 (MoO_4)_3$ nanocomposite. [C_0= 10.0 mg L^{-1}, pH = 6.0, dosage = 0.025 g, t_c = 5.0 min].

Dyes	T (^{O}K)	Kc	value of ΔG^o (kJ mol^{-1})	value of ΔH^o (kJ/mol^{-1})	value of ΔS^o (kJ mol^{-1} K^{-1})
(RhB) dye =10 (mg L^{-1})	288	-47.66	-95.58	-29.24	-131.49
	308	-57.4	-103.73		
	318	-96.33	-120.85		
	328	-145.0	-135.77		
	338	-291.0	-159.40		

Adsorption mechanism of (RhB) dye into Albizia Stem Bark Lebbeck modified by $Fe_2 (MoO_4)_3$ nanocomposite

The adsorption mechanism of the (RhB) dye onto the surface of the *Albizia Stem Bark Lebbeck* modified by $Fe_2 (MoO_4)_3$ nanocomposite can be inferred from the analysis of the IR results, in which the presence of functional groups (-O, MoO_4-, and Fe-O) on the surface was confirmed (Figure 7), shows the various potential interactions that may occur between the (RhB) dye and the *Albizia Stem Bark Lebbeck* modified by $Fe_2 (MoO_4)_3$ nanocomposite surface. Electrostatic interactions are favoured owing to the cationic nature of the dye with the negative surface charges of the *Albizia Stem Bark Lebbeck* modified by $Fe_2 (MoO_4)_3$ nanocomposite. The secondary interactions likely involve hydrogen bonding between the acceptor and the donor groups of the *Albizia Stem Bark Lebbeck* modified by $Fe_2 (MoO_4)_3$ nanocomposite – (RhB) dye system [45]. Along with π-π interactions that occur between the p–electron system of the *Albizia Stem Bark Lebbeck* modified by $Fe_2 (MoO_4)_3$ nanocomposite structure and the aromatic rings of the (RhB) dye molecules. In neutral and weak alkaline conditions, (RhB) dye exhibits substantial proton loss and exists as free ions in solution, thus inhibiting the chemical adsorption to some extent. However, structure of *Albizia Stem Bark Lebbeck* modified by $Fe_2 (MoO_4)_3$ nanocomposite, especially after modification, tempers the negative effect *via* physical adsorption [45,46].

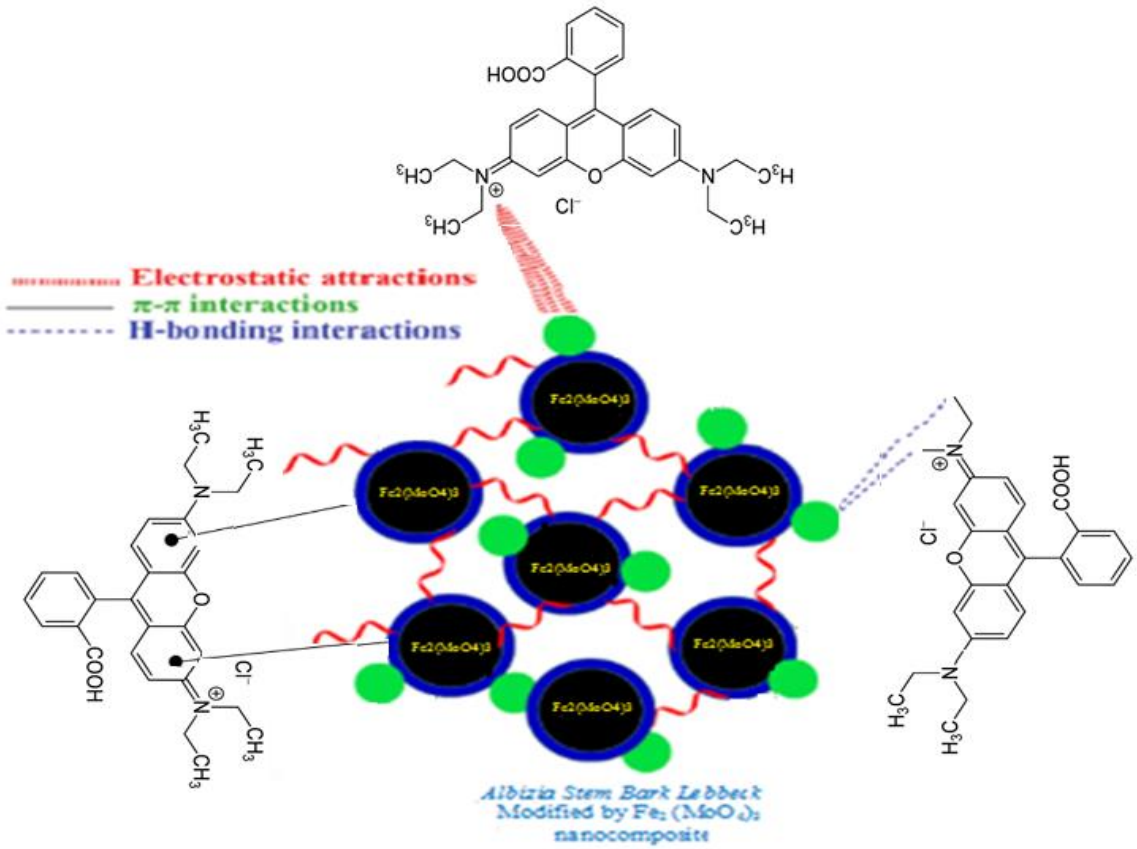

Figure 7. Illustration of the possible interaction between (RhB) dye and surface *Albizia Stem Bark Lebbeck* Modified by $Fe_2(MoO_4)_3$ nanocomposite.

Recycling of the Adsorbent

The ability of recovering and reusing of the adsorbent was tested in several steps of adsorption and the desorption process were done [44-47]. The results are shown in Figure 8. As shown in Figure 8, 99.0% of (RhB) dye was desorbed in the first run and after 6 runs, there were slight changes in (RhB) dye desorption. So, it was concluded that the desired removal of 99.0 % can be achieved after 6 runs.

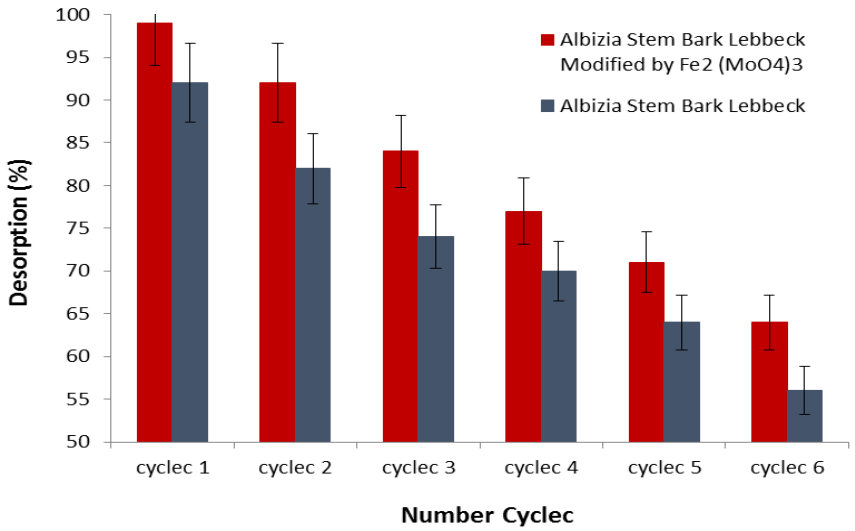

Figure 8. Desorption of (RhB) dye from *Albizia Stem Bark Lebbeck* Modified by $Fe_2(MoO_4)_3$ nanocomposite. [C_0= 10.0 mg L^{-1}, pH = 6.0, dosage = 0.025 g, t_c = 5.0 min, T=25^{0}C].

Comparison of various adsorbent

The performance of the proposed method has been compared with other adsorbents (Table 8). The adsorption capacity and contact time, superior to other adsorbents to remove (RhB) dye. The results indicated that the ultrasound-assisted removal method has are mark able ability to improve the efficiency of dyes removal. The ultrasonic-assisted enhancement of dye removal could be attributed to the high-pressure shock wave sand high speed micro jets during the violent collapse of cavitation bubbles.

Table 8. Comparison of results for this work with other reported.

Dye	Adsorbent	Dosage sorbent	pH	Time	Adsorption capacity	References
Rhodamine B (RhB)	Polymeric Dowex 5WX8 Resin	0.16 g	3.6	27.6 min	43.47 mgg^{-1}	[3]
Rhodamine B (RhB)	Kappaphycus alvarezii, Gracilaria salicornia and Gracilaria edulis	0.1 g	2.0	15 min	9.87, 11.03 and 97.08 mgg^{-1}	[7]
Rhodamine B (RhB)	$Zn(OH)_2$ -NPs-AC	0.025 g	4.0	4 min	76.38 mgg^{-1}	[8]
Rhodamine B (RhB)	waste of seeds of Aleurites Moluccana	2.0 g	5.5	120 min	117.0 mgg^{-1}	[15]
Rhodamine B (RhB)	Pomegranati Peel	0.1 g	6.0	25 min	7.37 mg g^{-1}	[36]
Rhodamine B (RhB)	*Albizia Stem Bark Lebbeck* Modified by $Fe_2(MoO_4)_3$ nanocomposite	0.025 g	6.0	5 min	98.0 mgg^{-1}	This work

Conclusion

The *Albizia Stem Bark Lebbeck* modified by $Fe_2(MoO_4)_3$ nanocomposite, has been synthesized and used as an effective adsorbent for the removal of (RhB) dye from aqueous solutions. Response surface methodology was exercised to design the experiments and quadratic model was utilized for the prediction of the variables. The excellent contribution of *Albizia Stem Bark Lebbeck* modified by $Fe_2(MoO_4)_3$ nanocomposite in deleting (RhB) dye was confirmed when the lowest errors were obtained in no time. On the other hand, some of advantages for this work are listed below:

Albizia Stem Bark Lebbeck plant is very inexpensive, energy saving, and the most important of all non-toxic. The use of waste *Albizia Stem Bark Lebbeck* modified by $Fe_2(MoO_4)_3$ nanocomposite sorbent as a natural and inexpensive valuable resource and environmentally benign support. According to the results, *Albizia Stem Bark Lebbeck* modified by $Fe_2(MoO_4)_3$ nanocomposite could be employed as a reusable adsorbent and would be an economically viable option that can lead to wastewater treatment advancement and high-quality treated effluent.

Acknowledgement

The authors gratefully acknowledge support of this work by the Islamic Azad University, Kermanshah Branch, Iran.

Conflict of interest

The authors declare that they have no conflict of interest related to the publication of this article.

References

[1] X. Tao, Sh. Wang, Zh. Li, *J. Environ. Manage.,* 255, 109834 (2020).

[2] L.P. Lingamdinne, J.R. Koduru, R.R. Karri, *J. Environ. Manage.,* 231, 622 (2019).

[3] M. Ali Khan, M. R. Siddiqui , M. Otero, Sh. Ahmed Alshareef, M. Rafatullah, *Polymers.,* 12, 500 (2020).

[4] F. Marahel, *Iran. J. Chem. Chem. Eng*., 38, 129 (2019).

[5] Y. Zhao, Zh. Li, *J. Mol. Liq.,* 293, 111516 (2019).

[6] F.H.M. Souza, V.F.C. Leme, G.O.B. Costa, K.C. Castro, T.R. Giraldi, G.S.S. Andrade, *Water Air Soil Pollut.,* 231, 1 (2020).

[7] A. Selvakumar, S. Rangabhashiyam, *J. Environ. Pollut.,* 255, 113291 (2019).

[8] M. Kiani, S. Bagheri, A. Khalaji, N. Karachi, *Desal. Water Treat.*, 226, 147 (2021).

[9] O.A. Adeleke, A. Ahmad, K. Hossain, M. Rafatullah, *J. Mol. Liq.*, 281, 48 (2019).

[10] S. Singh, N. Parveen, H. Gupta, *Environ. Technol. Innova.*, 12, 189 (2018).

[11] A.A. Abdulrazak, S. Rohani, *Adv. Mater. Sci. Eng.*, 2018, 1 (2018).

[12] H. Zeng, M. Gao, T. Shen, F. Ding, *Colloid. Surf. A.*, 555, 746 (2018).

[13] A.L.D. Da Rosa, E. Carissimi, G.L. Dotto, H. Sander, L.A. Feris, *J. Clean. Prod.*, 198, 1302 (2018).

[14] M. Tuzen, A. Sari, T.A. Saleh, *J. Environ. Manage.*, 206, 170 (2018).

[15] D.L. Postai, C.A. Demarchi, F. Zanatta, D.C.C. Melo, C.A. Rodrigues, *Alexan. Eng. J.*, 55, 1713 (2016).

[16] H. Esmaeilli, F. Foroutan, D. Jafari, *Korean. J. Chem. Eng.*, 37, 804 (2020).

[17] H. Pooladi, R. Foroutan, H. Esmaeili, *Environ. Monitor. Assess.*, 193, 1 (2021).

[18] M.M. Rashad, A.A. Ibrahim, D.A. Rayan, M.M.S. Sanad, I.M. Helmy, *Environ. Nanotechnol. Monit. Manag.*, 8, 175 (2017).

[19] R. Foroutan, S. J. Peighambardoust, S. Hemmati, *Int. J. Biolog. Macromol.*, 189, 432 (2021).

[20] G. Haghdoost, *J. Phys. Theore. Chem.*, 15(3,4), 141 (2019).

[21] F. Maghami, M. Abrishamkar, B. Mombeni Goodajdar, M. Hossieni, *Desal. Water Treat.*, 223, 388 (2021).

[22] M. Rahmani Piani, M. Abrishamkar, B. Mombeni Goodajdar, M. Hossieni, *Desal. Water Treat.*, 223, 288 (2021).

[23] S. Mahdi Hadi, M.K.H. Al – Mashhadani, M.Y. Eisa, *Chem. Ind. Chem. Eng. Q.*, 25, 39 (2019).

[24] S. Bagheri, H. Aghaei, M. Ghaedi, A. Asfaram, M. Monajemi, A.A. Bazrafshan, *Ultrason. Sonochem.*, 41, 279 (2018).

[25] F. Raoufi, H. Aghaee, M. Monajjemi, *Orient. J. Chem.*, 32, 1839 (2016).

[26] H.S. Ghazi Mokri, N. Modirshahla, M.A. Behnajady, B. Vahid, *Int. J. Environ. Sci. Technol.*, 12, 1401 (2015).

[27] M. Ullah, R. Nazir, M. Khan, W. Khan, M. Shah, S.G. Afridi, *J. Soil and Water Res.*, 15, 30 (2020).

[28] S. Rahdar, A. Rahdar, M.N. Zafar, S.S. Shafqat, S. Ahmadi, *J. Mater. Res. Technol.*, 8, 3800 (2019).

[29] G.K. Sharma, N. Dubey, A Review, *Int. J. Ayur. Herb. Med.*, 5, 1683 (2015).

[30] H.Z. Khafri, M. Ghaedi, A. Asfaram, M. Safarpoor, *Ultrason. Sonochem.*, 38, 371 (2017).

[31] M. Pargari, F. Marahel, B. Mombini Godajdar, *Desal. Water Treat.*, 212, 164 (2021).

[32] M. Kiani, S. Bagheri, N. Karachi, E. Alipanahpour Dil, *Desal. Water Treat.*, 152, 366 (2019).

[33] D. Nunez-Gomez, F. Lapolli, M. Nagel-Hassemer, M. Lobo-Recio, *Energy Proc.*, 136, 233 (2017).

[34] V. Kumar, P. Saharan, A.K. Sharma, A. Umar, I. Kaushal, Y. Al-Hadeethi, B. Rashad, A. Mittal, *J. Ceram. Int.*, 46, 10309 (2020).

[35] F. Marahel, B. Mombeni Goodajdar, N. Basri, L. Niknam, A.A. Ghazali, *Iran. J. Chem. Chem. Eng.*, 41, 1 (2022). doi: 10.30492/IJCCE.2021.527025.4636.

[36] Z. M. Saigal, A.M. Ahmed, *J. Chem.*, 21, 212 (2021).

[37] A. Azari, R. Nabizadeh, S. Nasseri, A.H. Mahvi, A.R. Mesdaghinia, *Chemospher.*, 250, 126238 (2020).

[38] A. S. Abdulhameed, A. K. Talaq Mohammad, A.H. Jawad, *Desal. Water Treat.*, 164, 364 (2019).

[39] M. Hubbe, S. Azizian, S. Douven, A Review. *Bio Resource.*, 14(3), 7582 (2019).

[40] R. Han, Y. Zhang, Y. Xie, *J. Separa. Purif. Technol.*, 234, 116119 (2019).

[41] A. Asfaram, M. Ghaedi, S. Hajati, A. Goudarzi, *Ultrason. Sonochem.*, 32, 418 (2016).

[42] N. Karachi, S. Motahari, S. Nazarian, *Desal Water Treat.*, 228, 389 (2021).

[43] N.N. Abd Malek, A.H. Jawad, A.S. Abdulhameed, K. Ismail, B.H. Hameed, *Int. J. Biolog. Macromol.*, 146, 530 (2020).

[44] Sh. Bouroumand, F. Marahel, F. Khazali, *Desal. Water Treat.*, 223, 388 (2021).

[45] A.H. Jawad, N.N.M. Firdaus Hum, A.S. Abdulhameed, M.Z. Mohd Ishak, *Int. J. Environ. Anal. Chem.*, 100, 1 (2020). https://doi.org/10.1080/03067319.2020.1807529.

[46] A.H. Jawad, I.A. Mohammed, A.S. Abdulhameed, *J. Polymers Environ.*, 28, 2720 (2020).

[47] F. Marahel, B. Mombeni Goodajdar, L. Niknam, M. Faridnia, E. Pournamdari, S. Mohammad Doost, *Int. J. Environ. Anal. Chem.*, 101, 1 (2021). https://doi.org/10.1080/03067319.2021.1901895.